Assessment of traffic-related PAH in various environmental components and its associated health risk at a highway Toll Plaza

Theres Charly*, Basavaraju Manu, Raviraj Mulangi

Department of Civil Engineering, National Institute of Technology Karnataka, Surathkal, Karnataka, India

ARTICLE INFORMATION

CORRESPONDING AUTHOR:

therescharly.197cv014@nitk.edu.in
Tel: (+91 824) 2473041
Fax: (+91 824) 2474033

ABSTRACT

Introduction: This study investigated Polycyclic Aromatic Hydrocarbon (PAH) emissions from road traffic at the Surathkal toll plaza, in Karnataka, India. It focuses on two phases: when the toll station operated (Phase 1: January 2020 – March 2020) and when it was inactive (Phase 2: January 2023 – March 2023).

Materials and methods: The research examines Suspended Particulate Matter (SPM) concentration, its elemental analysis, and various PAH concentrations in it during both phases. Ultrasonic extraction and Gas Chromatography (GC) analysis were used to study 16 priority PAHs recommended by the United States Environmental Protection Agency (US-EPA), identifying eight in samples like SPM, soot, and green leaves. Inductively Coupled Plasma Optical Emission Spectrophotometer (ICPOES) analysed 14 elements in SPM.

Results: Results revealed higher PAH concentration during Phase 2, indicating that the presence of toll structure negatively affects air quality even when inactive. In contrast, SPM and its elements had higher mean concentrations during Phase 1, suggesting an inverse relationship between SPM and PAH levels. PAH diagnostic ratios showed different sources for each phase, including gasoline, diesel, fossil fuel, coal/biomass, and pyrogenic sources. Comprehensive health risk assessment using BaP equivalent concentration (BaP_{eq}) to estimate Inhalation Life-time Cancer Risk (ILCR), revealed an increased risk during both phases (0.045 during Phase 1 and 0.134 during Phase 2), higher than acceptable risk level (1×10^{-6}).

Conclusion: This research underscores the toll plaza's significant influence on air quality and calls for the development of mitigation measures.

Introduction

Air pollution is a global concern, with traffic being a major contributor, encompassing both exhaust and non-exhaust sources. Among vehicle-emitted pollutants, Particulate Matter (PM) stands out as a significant health risk, associated with conditions such as lung cancer and respiratory diseases [1, 2]. PM is laden with hazardous compounds, notably Polycyclic Aromatic Hydrocarbons (PAHs), identified as carcinogenic [3, 4]. PAHs,

characterized by two or more fused benzene rings, primarily result from incomplete combustion of organic matter [5]. These complex compounds are found in various sources, including biomass burning, vehicular emissions, wood combustion, coal combustion, and industrial processes like steel production [6–8]. Vehicular emissions and coal combustion have been pinpointed as major sources of PAHs in India [9]. PAHs can be categorized into petrogenic PAHs, which are inherent components of fuels [10], and pyrogenic PAHs, formed through the pyrolysis or combustion of hydrocarbons [11]. The emission of pyrogenic PAHs from diesel engines is influenced by various operational conditions and fuel types [12, 13].

Toll plazas, integral components of road infrastructure, experience heightened pollutant concentrations due to increased fuel consumption during the deceleration-queuing-acceleration process [14]. As the vehicle approaches the toll plaza, it decelerates from its normal speed, remains in idling condition till the toll payment is done, and then accelerates back to its normal speed [15]. This change in driving patterns can result in the formation of hotspots near the toll plaza. Studies found that the emission of pollutants will be higher during the deceleration and acceleration process than idling condition [16], with the highest emission during acceleration [17]. To understand the phenomenon in a better way, this study was conducted in two phases, Phase 1: when the toll plaza was functioning i.e., the deceleration-idling-acceleration phenomenon takes space subsequently, and Phase 2: When the toll plaza was inactive i.e., deceleration of vehicle occurs due to the presence of toll structure followed by accelerating back to normal speed.

PM, composed of soot particles, soluble organic matter, ash, and other compounds, is a major contributor to air pollution from vehicle exhaust [18-20]. Soot which occurs from the collision of heavy PAH is a major concern for public health and the environment [21].

Because of the toxic nature of PAH, the United State Environmental Protection Agency (US EPA) has compiled 16 PAHs as priority pollutants among which 7 were categorized as carcinogenic i.e benzo[a]anthracene, benzo[k]fluoranthene, benzo- [a] pyrene, chrysene, benzo[b]fluoranthene, diben- z[a,h] anthracene and indeno [1,2,3-cd]pyrene [22, 23]. PAH can be divided into high molecular weight-PAH (HMW-PAH) and low molecular weight-PAH (LMW-PAH) depending on its molecular weight. PAHs with two or three rings can be categorized as LMW-PAH and those with four or more rings form HMW-PAH [24]. It is noteworthy to emphasize the growing significance of studies focusing on the detection of PAH in diverse environmental samples. Investigations about the presence of PAH in environmental mediums such as soil, airborne particulate matter, green plants, and food samples are gaining prominence within the realm of environmental research [25]. In recent years, research on air quality monitoring has focused on PAH due to its carcinogenic and mutagenic properties. The impact of PAH on human health depends on the concentration of PAH to which the individual is exposed, the length and route of PAH, and the toxicity of particular PAH. To evaluate the potential health risks linked to PAH, various methodologies have been devised, employing the concepts of Benzo (a) pyrene equivalent concentration (BaP_{eq}) and Toxicity Equivalent Factor (TEF) and are used by researchers [26].

Additionally, researchers recognized that green plants play a great role in absorbing and accumulating pollutants from the environment [27]. If the air in the area where plants are grown contains PAH, the leaves of the plants can have PAH accumulated in them depending on the surface characteristics like texture, waxy coating, etc. Trees and shrubs are more efficient than grassland in capturing PAH suspended in the air [28].

This study represents a pioneering investigation into the fluctuation of PAH levels across diverse

environmental components and the associated health risks attributed to traffic emissions, encompassing periods when the toll plaza functioned and during its non-operation. The study provides a valuable insight into the complex interactions between vehicular emissions, environmental factors, and human health risks associated with PAH exposure.

Materials and methods

This section describes the study area, the sampling procedure for air, leaves, soot, and incense sticks, the extraction of various samples, the procedure for PAH and SPM elemental analysis, and health risk assessment.

Study area description

Surathkal, situated along the Arabian Sea coast, is a vibrant suburb of Mangalore, Karnataka, India, known for its educational and industrial significance. Positioned to the north of Mangalore city, adjacent to National Highway 66, Surathkal experiences a tropical climate with hot and humid conditions from March to May, monsoon rains from June to October, and post-monsoon weather from November to February.

The focal point of this study, the Surathkal Toll Plaza, located at coordinates 13° 00' 45.8" N and 74° 47' 24.5" E, stands about 14 km south of Mangalore and 44 km north of Udupi. Figs 1a and b depict the location map and view of the study area, respectively. The toll plaza features six collection booths, three each for southbound and northbound toll collection, accommodating various types of vehicles from small cars to oversized vehicles. Toll collection methods include manual cash transactions and the FastTag system, with a peak capacity of 40,000 Passenger Car Units (PCU) as per the National Highway Authority of India (NHAI). The toll plaza operated until December 6, 2022.
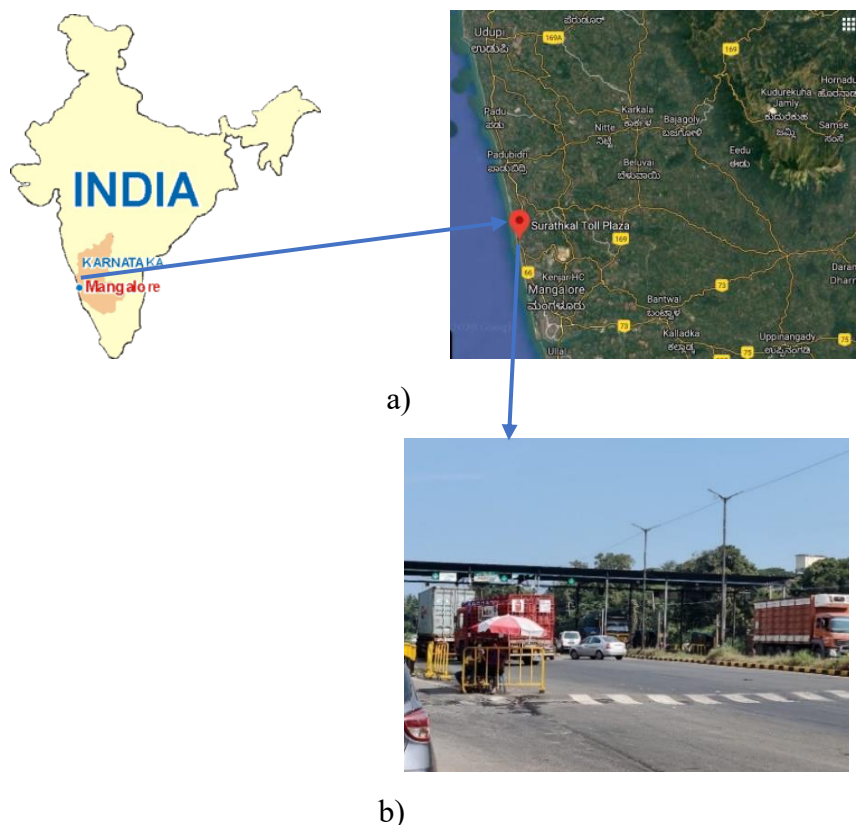

a)

b)

Fig. 1. a) Location map of Surathkal toll plaza (Google map); b) View of Surathkal toll plaza

The entire study period is categorized into two distinct phases. Phase 1 encompasses the period when the toll plaza was operational (January 2020 – March 2020), while Phase 2 corresponds to the period when the toll plaza remained inoperative (January 2023 – March 2023).

Sampling procedure

A comprehensive approach was adopted, encompassing the collection of representative samples from SPM, leaves, soot, and incense sticks, facilitating a thorough and precise analysis of PAH across diverse environmental matrices. The subsequent section details the sampling protocols employed for the various components.

Air Sampling

SPM samples were collected in accordance with Indian Standard (IS) 5182: Part 4 Methods for measurement of air pollution: Suspended Particulate Matter [29]. SPM was gathered using a High-Volume Sampler, (Respirable Dust Sampler, Polltech Instruments, Model: PEM-RDS-8NL), throughout the study and Glass microfiber filters, (MOLYCHEM, sized at 203 x 254 mm) were employed for the collection of these suspended particulates. Each filter paper underwent a meticulous inspection for any potential pinholes, particles, or imperfections. Filters exhibiting visible defects were excluded from use. Subsequently, the filter papers were accurately weighed to the nearest tenth of a milligram.

During the setup process, the glass fiber filters were positioned with the rough side facing upwards before initiating the instrument. Upon the completion of the sampling period, the filter retainer was cautiously removed from the filter holder, ensuring contact only with the outer edges. Sampling was done two to three times (alternate days except weekends) in all the week during both phases, and representative samples were carefully selected for subsequent PAH and elemental analyses. These sampling sessions were conducted for 8 h during daylight hours i.e.

from 9.00 am to 5.00 pm during both the phases. The instrument was positioned about 5 m away from the toll structure, with a height of 10 cm from the ground level.

Sampling of leaves

The chosen leaves for examination consisted of Napier grass (Pennisetum Purpureum) and Java plum (Syzygium Cumini), Hibiscus (Hibiscus rosa-sinensis) leaves, and leaves from the Rose apple tree (Syzygium jambos).

Leaf samples were gathered from in and around the toll plaza. Hibiscus leaves were collected from the eastern side of the study area (sampling location D), situated roughly 30 m from the toll structure, while the leaves of the rose apple tree were obtained from the western side of the study area, approximately 10 m from the structure (sampling location C). Napier grass was collected from a site near the toll plaza(sampling location B), whereas Java plum leaves were sourced from a residential yard located approximately 100 m towards the eastern side of the study area(sampling location A). Notably, the Java plum leaves displayed visible black spots on their surfaces, which raised suspicions of potential contamination from a nearby petroleum industry. Consequently, the sampling encompassed a range of environments, including residential areas, academic zones, and roadside sections of the institution.

To ensure consistency, the leaf samples collected were of uniform size, and maturity, and exhibited healthy appearances to the extent possible. These leaves were harvested at a height ranging from 0.5 to 1.0 m above ground level. Subsequently, the collected leaves were placed in plastic trays and transported to the laboratory. Upon arrival, they underwent a process of oven drying and were then finely ground into a powder for analysis.

Sampling of soot and incense stick

Soot samples were gathered from a divider located within a 5-m radius of the toll plaza. To guarantee uniformity, the collection encompassed

four distinct sites, including two samples from each side of the toll plaza. These samples were meticulously scraped and accumulated onto small plates. Additionally, incense stick samples were procured from the residential area near the toll plaza. Subsequently, the powdered samples were securely stored in a tightly sealed glass container within a freezer set at -18°C, awaiting extraction and analysis

Analysis of mass concentration of SPM

The determination of SPM mass concentration was conducted through the gravimetric approach, by IS 5182: Part 4 - Methods for measurement of air pollution: Suspended Particulate Matter [29] guidelines. This method relied on measuring the initial and final weight of the filter paper, which were quantified in grams (g) using a precision weighing balance (Accuracy: 0.0001 g), along with the volume of air sampled expressed in (m³).

Extraction of sample

Samples were subjected to extraction processes to detect the existence and quantify the concentration of PAH within diverse compounds and to conduct an elemental analysis of SPM. PAH analysis was done for all the 16 priority pollutants and their characteristics are given in Table 1.

Table 1. Characteristics of 16 prioritized PAHs [30]

PAHs	Abbreviation	Molecular mass(g/mol)	Carcinogenic group*	TEF	Number of rings
Naphthalene	NPH	128	D	0.001	2
Acenaphthylene	ACY	152	D	0.001	3
Acenaphthene	CAN	154	NA	0.001	3
Fluorene	FLU	166	D	0.001	3
Phenanthrene	PHN	178	D	0.001	3
Anthracene	ATR	178	D	0.01	3
Fluoranthene	FLT	202	D	0.001	4
Pyrene	PYR	202	NA	0.001	4
Benzo[a]anthracene	B[a]A	228	B2	0.1	4
Chrysene	CHR	228	B2	0.01	4
Benzo[b]fluoranthene	B[b]F	252	B2	0.1	5
Benzo[k]fluoranthene	B[k]F	252	B2	0.1	5
Benzo[a]pyrene	B[a]P	252	D	1	5
Indeno[1.2.3-cd]pyrene	I[123-cd]P	276	B2	0.1	6
Dibenz[a,h]anthracene	D[ah]A	278	B2	1	5
Benzo[g,h,i]perylene	B[ghi]P	276	B2	0.01	6

*B2: possibly carcinogenic to humans, D: unclassifiable to carcinogenicity, and NA: Not available

SPM for elemental analysis

SPM, which was collected using Glass microfiber filters, underwent analysis for fourteen distinct elements: Ag, Al, Ba, As, Cr, Mn, Ni, Cu, Pb, Th, Se, Zn, V, and Fe. The assessment of these elements in SPM involved a digestion process adhering to the USEPA standard operating procedure compendium io-3.1 [31]. The methods described Quality Control and Quality Assurance (QC/QA) procedures were adhered to. The method employed for metal extraction from the filter paper was a hot plate digestion technique. In summary, the filter paper was cut into 1 x 8-inch segments, and 10 mL of an extraction solution was added. To prepare the extraction solution, 167.5 mL of concentrated HCl and 55.5 mL of concentrated HNO_3 were combined with 500 mL of de-ionized water and thoroughly mixed. This mixture, along with the filter paper, underwent reflux at 90°C for 30 min without boiling. After the extraction, the sample was allowed to return to room temperature for 30 min, followed by the addition of 30 mL of de-ionized water. The solution was then filtered using a 0.22 μm syringe filter and adjusted to a total volume of 40 mL with de-ionized water. Similar digestion procedures were applied to blank filters. The concentration of trace elements was quantified using an Inductively Coupled Plasma Optical Emission Spectrometer (ICP-OES) from Agilent Technologies, aligning with the USEPA standard operating procedure compendium io-3.5 [32]. This method enabled the multi-element determination of trace elements. The final concentration was determined by subtracting the concentration of the blank from that of the samples.

SPM for PAH analysis

Particle and gas-phase PAHs were extracted from the SPM collected on filter paper, following the procedures outlined in IS 5182 Method for Measurement of Air Pollution Part 12: PAHs in Air Particulate Matter [33]. In summary, half of the exposed filter paper was cut into small strips within a beaker, and 100 mL of toluene was introduced for the extraction process. This mixture was then subjected to a 30-min treatment in an ultrasonic bath, and the resulting extract was filtered through Whatman filter paper No. 20. This extraction process was repeated twice, and the collected extracts were combined. Subsequently, a clean-up and enrichment procedure was carried out using a silica gel column measuring 200 mm in length and having an internal diameter of 0.5 cm. After conditioning, the extract was introduced at the upper end of the silica column. All PAH compounds were captured using 5 mL of cyclohexane and collected into a rotary evaporator flask, where they were subsequently reduced to a volume of approximately 1 mL. This concentrated extract was then transferred to a vial and stored in a dark, cool environment before the analysis phase.

Leaves, soot, and incense stick samples for PAH extraction

PAHs were extracted from leaf, soot, and incense stick samples employing the ultrasonic extraction method (Fig. 2). In this process, 12 g of each type of sample were placed within a 250 mL vial, with the addition of 50 mL of Dichloromethane (DCM) to each vial. These sealed vials were then subjected to ultrasonic extraction in a bath at 30 °C for 30 min, and the resulting extracted fraction was collected. This extraction cycle was repeated three times. Subsequently, the DCM layers were amalgamated and evaporated on a rotary evaporator at 30 °C. The resulting residue was dissolved in 2 mL of n-hexane and subjected to purification through silica-gel column chromatography. Before this, the column was preconditioned with a 10 mL solution of DCM and n-hexane (50:50). The same solvent mixture (50 mL) was used for eluting the PAHs. The purified extract was then concentrated to near dryness using a rotary evaporator operating at 30 °C. The resulting residue was subsequently dissolved in 2 mL of DCM, followed by filtration using a 0.45 mm syringe filter before undergoing analysis by Gas Chromatography (GC). It is noteworthy that DCM was selected for its lower boiling point compared to all 16 PAHs, a choice that has been adopted by various researchers in their studies [34].

(a)   (b)   (c)
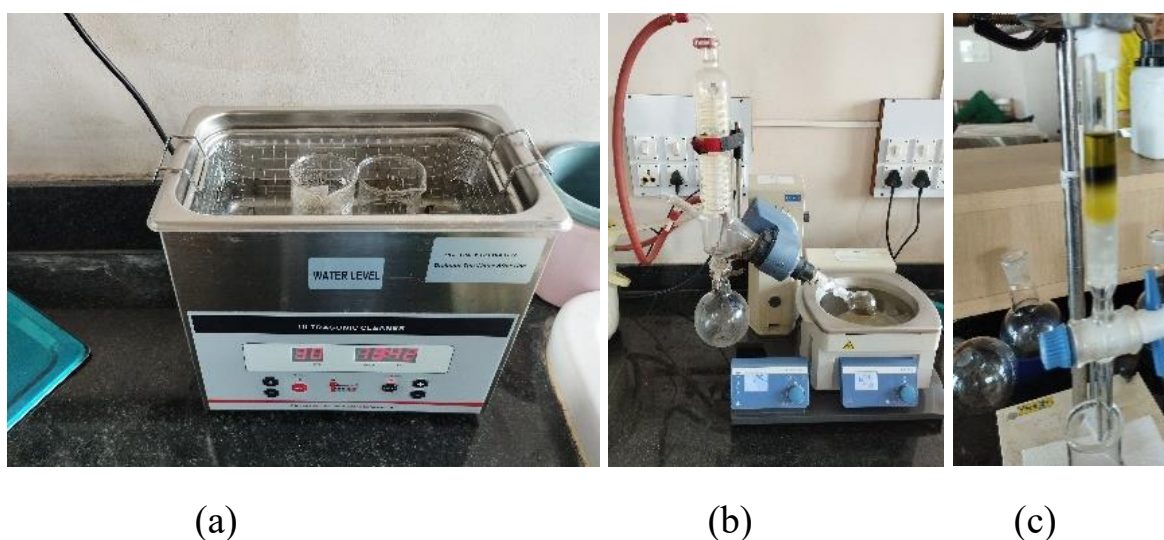
Fig. 2. a) Beaker with sample kept in an ultrasonic bath, b) Filtered extract kept in a rotary evaporator, c) Silica gel column chromatography

GC analysis

Each extract underwent analysis utilizing the NETEL Microprocessor-Based Gas Chromatograph Model MICHRO 9100, following the IS 5182 Method for measurement of Air Pollution Part 12: PAHs in Air Particulate Matter [33] guidelines. A 1µl portion of each sample was introduced in split-less mode at an injection temperature of 320°C, with a MEGA-PAH capillary column (20 m X 0.18 X 0.18 µ). Initially, the GC oven was heated to 130°C and subsequently increased at a rate of 6°C /min for 4 min, followed by a faster rate of 10°C/min for 5 min. The carrier gas employed was nitrogen at a flow rate of 1 mL/min. Each sample underwent a runtime of approximately 45 min.

To enable the quantification of PAH, the GC instrument was meticulously calibrated utilizing a standard PAH mix (610 PAH calibration mix A) sourced from Restek, US. This reference material encompassed the 16 US EPA-specified PAH compounds, as detailed in Table 1.

Quality assurance/Quality control (QA/QC)

The High-Volume Sampler underwent calibration by the manufacturer (Polltech Instruments Pvt. Ltd, Mumbai, India) before the study commencement. Prior to sample analysis, the spectrophotometer underwent self-calibration. The sampling and analysis procedures for SPM were conducted in accordance with the Indian Standard code [29] and USEPA guidelines [35]. Filter papers were maintained at a constant temperature (24±3°C) both before and after sampling, and they were handled with care during transportation to prevent background contamination. Elemental and PAH analysis of SPM adhered to the QA/QC protocols specified by USEPA [30–32].

Source identification using diagnostic ratio

Diagnostic ratios form a major tool in identifying the main source of pollutants. The method includes comparing the value obtained in the study with the value obtained from other literature [36, 37]. To find the possible source of PAH in the study, the following diagnostic ratios were used: FLU/

(FLU+PYR), FLT/(FLT+PYR), and PYR/B[a]P. The ratio LMW-PAH/HMW-PAH was also used to determine the pollution source.

Health risk assessment

The potential health risk of various PAHs was quantified using the concept of BaP equivalent concentration (BaP$_{eq}$) and Inhalation Life-time Cancer Risk (ILCR) given in (Eq. 1) and (Eq. 2) respectively.

$$BaP_{eq} = \sum(C_i \times TEF_i) \tag{1}$$

$$ILCR = UR_{BaP} \times BaP_{eq} \tag{2}$$

Where,

C_i =Concentration of individual PAH in ng/m³

TEF_i =Toxic Equivalent Factor of each PAH given in Table 1

UR_{BaP} =Unit lung cancer risk of BaP$_{eq}$.

UR_{BaP} denotes the population at risk due to the inhalation of BaP$_{eq}$. The value used in this study is 8.7×10^{-5}, which is observed in air quality guidance reported by the World Health Organization (WHO) in 2000 [38] and used by [39] and [40].

Results and discussion

The present study investigates variations in SPM concentration, the elemental composition of SPM, and PAH levels within different environmental components under both active and inactive periods of a toll plaza. Furthermore, the research delves into the evaluation of health risks associated with the identified PAHs.

Mass concentration of SPM

The average mass concentration of suspended particulate matter fell within the range of 250.00 µg/m³ to 350.00 µg/m³ in phase 1, with the highest recorded concentration at 411.864 µg/m³ and the lowest at 139.216 µg/m³ in January 2020. Similarly, during phase 2, the mean mass concentration of SPM ranged from 285.071 µg/m³ to 305.568 µg/m³, with the highest level observed at 410.805 µg/m³ and the lowest at 101.171 µg/m³ in February 2023. However, it is worth noting that when compared to the National Ambient Air Quality Standards (NAAQS), the concentration of SPM exceeded the permissible limits on all days in both phases. The extent of this increase in particulate matter concentration was influenced by factors such as traffic volume, delays, and prevailing meteorological conditions, which aligns with findings from a study conducted by [41]. Additionally, when examining the mean mass concentration of SPM, it was observed that the concentration of SPM generally decreased during phase 2, except during the pre-monsoon season, primarily due to the implementation of lockdown measures in March 2020 (as shown in Table 2).

Variations in the concentration of SPM revealed the variation in air quality during different operational phases. The presence of SPM served as an indicator of air quality. The concentration of air pollutants was higher during Phase 1, corresponding to the operational condition of the toll plaza when vehicles were idling frequently and emitting higher concentrations of pollutants. In contrast to phase 1, phase 2 characterized by the continuous flow of vehicles eliminating the idling period improves the air quality by emitting less concentration of SPM.

Elemental composition of SPM

During the elemental analysis of SPM collected when the toll plaza was operational, fourteen elements - Ag, Al, Cr, Cu, Mn, Ba, Ni, Pb, As, Th, V, Se, Zn, and Fe were detected in varying quantities. Similarly, in samples collected during the non-functioning period, ten elements - Ag, Cr, Al, Cu, Mn, Ba, Ni, Mn, Pb, V, Th, Zn, and Fe were identified (Fig. 3).

Table 2. The mean mass concentration of SPM ($\mu g/m^3$) and its percentage decreased during the study period

Sampling period	Phase 1 (Year: 2020)	Phase 2 (Year: 2023)	% decrease
January	339.75 ± 67.58	285.07 ± 40.99	16.09
February	339.51 ± 18.24	301.66 ± 68.64	11.15
March	275.21 ± 33.88*	305.57 ± 29.69	-11.03

*Low concentration of SPM due to imposition of lockdown due to COVID-19.
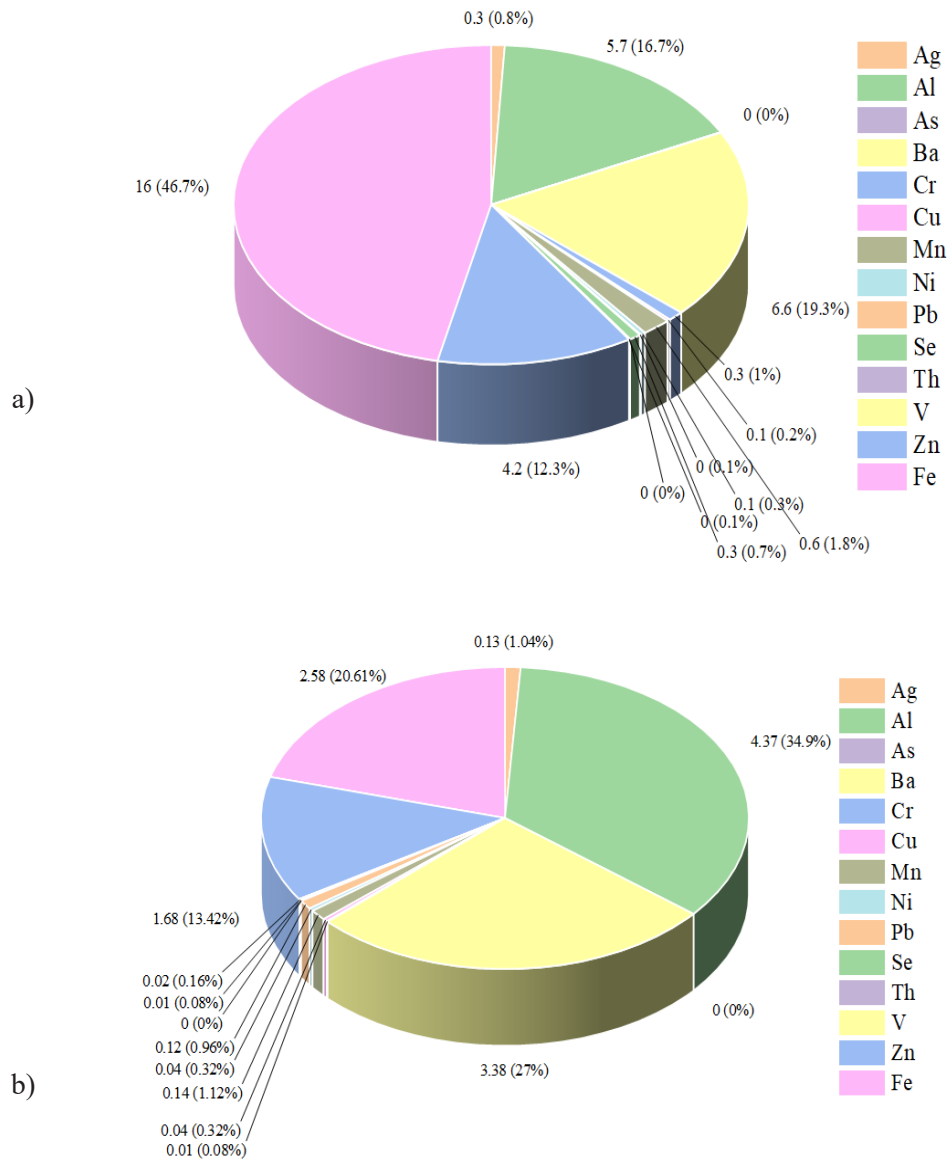

Fig. 3. Variation in concentration of elements in SPM during: a) Phase 1; b) Phase 2

Comparing the element concentrations, it's noteworthy that the presence of Fe was notably higher when the toll was operational, and it decreased by 84% during the period when the toll plaza was not functioning. Among all the elements, only As and Se were observed during the operational phase. In terms of quantity, during Phase 1, Fe had the highest weight percentage at 46.7%, followed by Ba, Al, and Zn. In Phase 2, Al held the highest weight percentage at 34.9%, followed by Ba, Fe, and Zn. These elemental signatures indicate the contribution of non-exhaust vehicular emissions. The elevated concentrations of Fe and Ba are likely associated with brake wear, while Zn is attributed to tire wear. The higher concentration of Al may result from re-suspension due to tire abrasion, wind, and vehicle turbulence,

as explained by researchers [42].

PAH analysis in SPM

Table 3 depicts the varying concentrations of diverse PAHs found in SPM at toll plazas during the study period. The collective concentration of PAHs in SPM exhibited a range from 699 to 8384 (mg/m^3).

Within SPM, the presence of 4 and 5-ringed PAHs was observed, which were notably prominent in their distribution, particularly during Phase 2, where they accounted for 81% to 100% of the entire PAH profile. The concentration of distinct PAHs identified during Phase 1 displayed a variation from 28 mg/m^3 to 476 mg/m^3, cumulatively amounting to 699 mg/m^3.

Table 3. Mean concentration and frequency of detection of PAH in SPM during Phase 1 and Phase 2

PAH	Phase 1		Phase 2	
	Mean(mg/m^3)	Frequency of detection (%)	Mean(mg/m^3)	Frequency of detection (%)
PYR	81	100	1025	100
PHN	81	100	200.67	67
B[k]F	28	100	170.33	100
B[a]P	476	100	875.67	100
D[a,h]A	33	100	516	100
FLT	0	0	2243.67	100
B[a]A	0	0	1282.67	67
FLU	0	0	315	33

In total, the study identified the presence of 8 PAHs in the vicinity of the toll plaza. PYR, PHN, B[k]F, B[a]P, and D[a.h]A were found during phase 1, and PYR, PHN, B[k]F, B[a]P, FLT, B[a]A, FLU, and D[a,h]A were found during phase 2 in SPM. The highest incidence of PAHs was detected in SPM during both phases. This can be due to the aerodynamic diameter of PM which favors the presence of HMW-PAH such as PYR, B[k]F, B[a]P, FLT, B[a]A, FLU and D[a.h]A [43,44]. It's noteworthy that the SPM concentration was higher during Phase 1 when the toll plaza was operational. In contrast, the concentration of PAHs was greater during Phase 2, corresponding to the period when the toll plaza was not operational. It's worth noting that previous research has also highlighted an interesting trend: a higher total of PAHs is associated with lower concentrations of Particulate Matter (PM), as observed in the study by researchers [43].

PAH analysis in leaf samples

Java plum leaves revealed only the presence of D[a,h]A, a 5-ringed PAH recognized by the WHO Joint Expert Committee on Food Additives (JECFA) as genotoxic and carcinogenic. This PAH is likely to be emitted from the exhaust condensate of gasoline engines. Given the prevailing daytime wind direction from the sea to the land (west to east concerning the toll station), and the fact that Napier grass and java plum leaves were collected from the eastern side of the campus, it is plausible that the PAHs detected resulted from the deposition of pollutants carried by the wind from the toll plaza. Intriguingly, no PAHs were detected in the Napier grass sample, which is consistent with the wide variation in PAH concentrations in Napier grass, influenced by factors like cultivation methods, harvesting, processing, and storage.

On the other hand, leaves collected from the western side of the study area exhibited a more significant number of PAHs, including PYR, PHN, B[a]P, D[a,h]A, FLT, and B[a]A. Notably, B[k]F predominated in rose apple leaves, followed by D[a,h]A and B[a]A, with respective concentrations

of 2606 mg/m^3, 955 mg/m^3, and 613 mg/m^3 (Fig. 4).

In the hibiscus leaf sample, PYR emerged as the most abundant of the quantified PAH, constituting 37.94% of the total PAH content. Furthermore, the hibiscus leaf sample displayed the presence of 4-ringed PAH (FLT) and 3-ringed PAH (PHN).

Within all three sampling locations, D[a,h]A was the exclusive HMW-PAH identified. Notably, the highest concentration of D[a,h]A was observed in the sampling location C, amounting to 955 mg/m^3, whereas the lowest concentration was recorded in the sampling location A, measuring 24 mg/m^3. D[a,h]A, a 5-ringed HMW-PAH observed in all the samples (SPM, soot, all leaf samples except Napier grass) is related to heavy traffic sources [9, 43].

When considering the total mass concentration of all the identified PAHs, the leaves of the rose apple tree accumulated the highest PAH levels, followed by hibiscus and java plum leaves. This trend reflects the higher PAH concentrations in roadside samples compared to the other two locations. It's worth noting that the concentration of PAH in Napier grass was below the detectable limit, underscoring that trees and shrubs accumulate more PAHs than grassland.

The data representing each sampling location category exhibited a notable degree of dispersion, signifying variations in the concentration of individual PAHs. In particular, the sampling location A displayed lower PAH concentrations when compared with other two locations.

PAH in soot sample

This section delves into the fluctuations in the concentration of various PAHs within soot samples in the study area during both Phase 1 and Phase 2. It sheds light on the influence of the toll structure on PAH concentrations, even during periods when the toll plaza was inactive.

Soot samples obtained from the vicinity of the

divider near the toll station exhibited the presence of PYR, (B[a]P), and D[a,h]A while the toll was operational. In Phase 2, four additional PAHs, namely PHN, B[k]F, FLT, and B[a]A, were identified in the soot sample (Table 4). Notably, the concentration of all the detected PAHs was higher during Phase 2. This observation might be attributed to the deceleration-acceleration process as opposed to a deceleration-queuing-acceleration process. The presence of PYR, FLT, and B[k]F is due to the burning of gasoline and diesel by vehicles which will be more during the deceleration-acceleration process [43, 44]. Therefore, the concentration of PAH will be higher during slow-moving conditions. This conclusion is supported by the findings of [45] that heavy vehicles moving at slow speeds emit higher concentrations of PAH into the atmosphere.
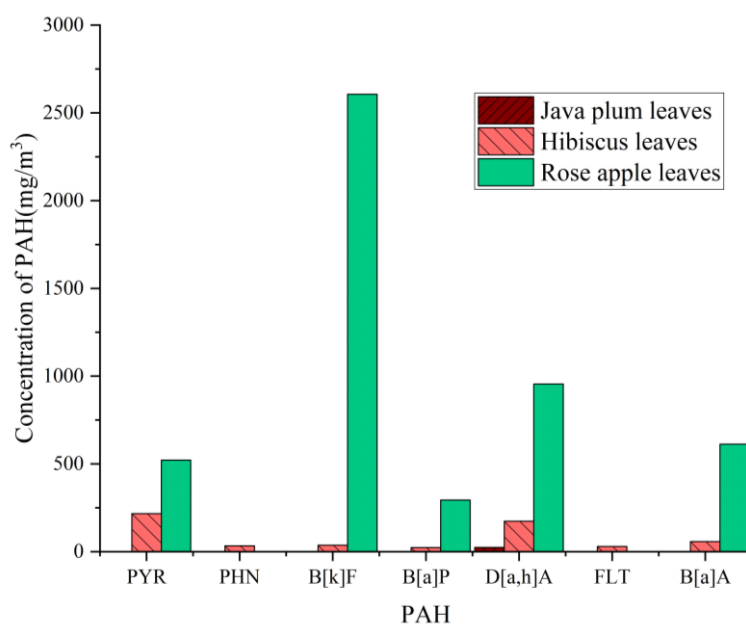

Fig. 4. Concentration of PAH in leaves samples

Table 4. Mean concentration and frequency of detection of PAH in soot during Phase 1 and Phase 2

PAH	Phase 1		Phase 2	
	Mean(mg/m^3)	Frequency of detection (%)	Mean(mg/m^3)	Frequency of detection (%)
PYR	51	100	547	100
PHN	0	0	70.5	100
B[k]F	0	0	78	100
B[a]P	31	100	250	100
D[a,h]A	29	100	249	100
FLT	0	0	557.5	50
B[a]A	0	0	27.5	50
FLU	0	0	0	0

The presence of the toll structure and road humps before and after the toll structure led to an increase in PAH concentration in soot samples, elevating it from 111 mg/m³ to 1779 mg/m³. Interestingly, the concentration of D[a,h]A) decreased from 29 mg/m³ (in soot) to 24 mg/m³ (in java plum leaves) with a lateral distance of approximately 200 m between the toll and leaf sample collection area during the toll's operation.

During Phase 2, the average concentration of total 4-ringed PAHs was approximately twice that of 5-ringed PAHs and roughly sixteen times that of 3-ringed PAHs. Additionally, the concentrations of 4-ringed and 5-ringed PAHs fell within a similar range (50-60 mg/m³), with no LMW-PAHs detected during Phase 1.

PAH in incense stick sample

Although the incense stick sample, which burned inside a living area, was initially chosen as a control, the analysis of the collected sample revealed the existence of a four-ring PAH known as PYR and a five-ring PAH called B[a]P. Notably, these HMW-PAHs were also identified in SPM and soot samples, with the highest concentration observed in SPM, followed by soot and incense sticks.

PAHs diagnostic ratio used as a source indicator

Table 5 shows a comparison between PAH diagnostic ratios of SPM and soot for the study area during two phases. These diagnostic ratios are instrumental in discerning the sources of various pollutants, including those stemming from diesel engines, gasoline engines, fossil fuel combustion, coal, biomass combustion, etc [39, 43]. Specific PAHs serve as indicators of particular emission sources in the environment [37]. For example, the diagnostic ratio FLU/(FLU+PYR) can be used to distinguish between diesel and gasoline.

FLU/(FLU+PYR) > 0.5 has been used for diesel emissions and FLU/(FLU+PYR) <0.5 for gasoline emissions [44]. In the present study, this diagnostic ratio was found to be <0.5 (0.24), which is characteristic of gasoline emission. The PYR/B[a]P diagnostic ratio, used to distinguish between diesel and gasoline emissions, exhibited values of 0.17 and 1.17 for SPM and 1.65 and 2.19 for soot during Phase 1 and Phase 2, respectively, indicating gasoline as the primary pollution source [37]. Additionally, the FLT/(FLT+PYR) ratio below 0.4 is indicative of petrogenic emissions, while ratios between 0.4 and 0.5 (as observed in soot during Phase 2) suggest the net combustion of fossil fuel. Ratios >0.5 (also observed in SPM during Phase 2) indicate coal and biomass combustion[40,43,46]. The ratio of LMW-PAH (PHN+FLU) to HMW-PAH (PYR+B[k]F+B[a]P+ D[a,h]A+FLT+B[a]A) calculated to be <1, indicates a pyrogenic nature of emission sources [36]. In terms of FLT/PYR, our results did not align with the diagnostic ratio. This can be due to the influence of some other factors affecting the ratio. According to the reference values, the PAHs originated from gasoline, diesel combustion and pyrogenic source during phase 1 and from gasoline engine, net combustion of fossil fuel, coal/biomass combustion, diesel combustion and pyrogenic sources during phase 2.

Analyzing the diagnostic ratios of PAH in hibiscus leaf samples (samples in which the highest number of PAHs were observed), PYR/B[a]P has a value of 9.43 signifying that the predominant source of PAH emissions was from diesel engines [37]. This conclusion is supported by the fact that these samples were collected close to the parking area in front of the academic area. Furthermore, the FLT/(FLT+PYR) ratio in green leaves exhibited a value of 0.12, which is <0.4, indicating a petrogenic source of pollution. However, the LMW-PAH/HMW-PAH ratio, exceeding 1, signified a pyrogenic source of pollution.

Table 5. Diagnostic ratios of PAH in SPM and soot during Phase 1 and Phase 2

Diagnostic ratio	SPM		Soot		Reference value	Source	Reference
	Phase 1	Phase 2	Phase 1	Phase 2			
FLU/(FLU+PYR)	0	0.24	0	0	>0.5	Diesel	[37,43,44]
					<0.5	Gasoline	
PYR/B[a]P	0.17	1.17	1.65	2.19	~ 10	Diesel engine	[37]
					~1	Gasoline engine	
FLT/(FLT+PYR)	0	0.69	0	0.50	<0.4	Petrogenic	[43][40][46][39]
					0.4–0.5	Net combustion of fossil fuel	
					>0.5	Coal/biomass combustion	
C-PAH/T-PAH*	0.84	0.55	0.74	0.51	~1	Diesel Combustion	[37]
LMW-PAH/ HMW-PAH	0.13	0.84	0	0.04	>1	Petrogenic	[36,47]
					<1	Pyrogenic	

*Sum of major non-alkylated compound (FLU + PYR + B[a]A + B[k]F + B[a]P)/Total concentration of PAHs.

Table 6. BaP$_{eq}$ and ILCR of PAHs in SPM and soot during Phase 1 and Phase 2

	SPM		Soot	
	Phase 1	Phase 2	Phase 1	Phase 2
BaP$_{eq}$	511.962	1540.751	60.051	510.725
ILCR	0.045	0.134	0.005	0.044

Health risk of PAHs

Among the 8 PAHs identified, B[a]P, D[a,h]A, B[k]F, and B[a]A are considered to be probable human carcinogens from the carcinogenicity of PAHs reported in Table 1. Notably, our findings indicate that a significant portion of the PAHs present in the samples collected during both Phase 1 and Phase 2 (ranging from 42% to 67%) exhibit carcinogenic properties. The results from Table 3 and Table 4 indicate that D[a,h]A has the highest contribution towards BaP$_{eq}$ other than B[a]P indicating a relatively higher risk than other PAHs. Table 6 further reveals that the highest BaP$_{eq}$ values were observed in SPM during Phase 2, whereas the lowest values were recorded in soot during Phase 1. This discrepancy can be attributed to the varying concentrations of D[a,h]A and B[a]P, with SPM having higher levels during both phases.

Table 6 highlights that the ILCR values in both SPM and soot samples collected during both phases exceed the "acceptable risk" threshold (1×10^{-6}) as stipulated by WHO[38]. Notably, the most elevated ILCR value (0.134, signifying that out of 1000 individuals exposed to the Phase 2 conditions throughout their lifetime, 134 cancer cases are expected to develop) was observed in SPM during Phase 2. These results indicate that both the deceleration-queuing-acceleration process (Phase 1) and the deceleration-acceleration process (Phase 2) pose a significant risk to individuals exposed to these conditions.

Conclusion

The study prominently illustrated the variations in SPM mass concentration and its corresponding elemental analysis during the two distinct phases. The investigation delved into the concentrations of PAHs, encompassing both HMW-PAH and LMW-PAH compounds, in samples derived from SPM, leaves, soot, and incense sticks. This is the first study assessing the variation in concentration of PAH in different components of the environment due to the presence of toll plazas.

From the results of this study, the following conclusions can be drawn:

1.   During Phase 1, there was a notable increase in the mean mass concentration of SPM and the identified elements, attributed to the additional waiting and idling phases associated with toll payment. Phase 2 exhibited higher concentrations of PAHs, attributed to the deceleration-acceleration cycle without queuing and stopping in between. This trend was consistently observed across various types of samples. An inverse relationship was observed between the mean mass of SPM and the concentration of PAHs, indicating that as SPM decreases, PAH concentrations tend to increase.

2.   The average total concentration of 4-ring PAHs was higher during Phase 2 in both SPM and soot samples when compared to 3-ring and 5-ring PAHs. However, during Phase 1, the highest concentration in SPM was observed for 5-ring PAHs, while in soot samples, the concentration of 4-ring and 5-ring PAHs fell within the same range. Additionally, two compounds, namely FLT and B[a]A, were detected in both SPM and soot samples during Phase 2. Moreover, a 3-ring PAH, FLU, was identified in SPM samples during Phase 2, a presence not observed in other sample types. Detection of HMW-PAH(e.g., B[a]P and D[a,h]A) in the samples indicates potential sources of these compounds in the environment, such as vehicle emissions.

3.   PAH concentrations in leaves collected from various regions within the study area showcased variations in pollutant concentration. The highest concentration was observed in roadside samples collected near the toll structure. Notably, only a single 5-ring PAH was detected in samples collected from the residential area, while HMW-PAHs constituted the highest percentage in leaves collected from the academic area. Some samples, like Napier grass, did not contain detectable levels of PAHs, suggesting that the presence of PAHs in vegetation samples can vary based on factors such as the type of vegetation and local environmental conditions. Also, the presence of PAH in various samples like SPM, soot, leaves, and incense sticks burned inside a living area suggests that PAHs are prevalent in both indoor and outdoor environments.

4.   Meteorological factors such as wind direction, particularly the movement of air from the sea toward the land (west to east concerning the toll station), may have influenced the distribution of PAHs, with samples collected from specific areas showing higher PAH concentrations.

5.   The presence of the toll structure and road humps before and after the toll plaza led to increased PAH concentrations in soot samples, highlighting the potential impact of traffic volume and infrastructure on PAH levels. Important insights were obtained from soot samples and leaves of different plant species, confirming the

impact of parking lots and toll booths on the PAH composition.

6. Analysis of diagnostic ratios of PAH in various environmental matrices such as SPM, soot, and leaves offers valuable insight into the sources of PAH emission. This study has revealed that, during Phase 1, the primary sources of PAHs are gasoline and diesel engine combustion, along with pyrogenic sources, while in Phase 2, major contributions stem from fossil fuel combustion, gasoline engines, coal/biomass burning, pyrogenic emissions, and diesel engine operation.

7. The ILCR values calculated for the environmental matrices served as indicators of cancer risk associated with exposure to traffic-related conditions. This research underscores the significance of recognizing and ameliorating the pollution sources that contribute to health risks, particularly in areas characterized by high vehicular emissions.

8. This research holds significant relevance in assessing the degree of contamination within diverse environmental components due to vehicular activity near toll structures. It provides valuable insights into the degradation of air quality concerning PAHs resulting from traffic movement, especially in proximity to educational institutions.

By identifying the source of PAH in the vicinity of the toll plaza, the study raises awareness among society about the environmental impact of emissions from vehicles. Also identifying the specific source of pollution helps in adopting mitigation measures. With the identification of pollution sources such as gasoline and diesel engines, the study offers insight to environmental agencies and policymakers to make regulations and strategies to control air pollution and thus enhance the air quality in toll plazas and transportation hubs. Achieving this goal could involve initiatives such as implementing green infrastructure, promoting the adoption of electric and hybrid vehicles, and establishing new emission standards.

The study provides insights into the distribution, sources, behaviour of PAHs, and diagnostic ratios of PAH in the study area, particularly in the context of the toll plaza and its associated environmental impact. External factors such as meteorological variables and variations in traffic volume are not considered extensively in the present study. Further analysis and investigation based on these parameters may be needed to explore the specific sources and implications of PAHs in the study region. Also, due to the volatile nature of LMW-PAH, the concentration of certain PAHs was below the detectable limit.

Ethical considerations

Ethical issues (Including plagiarism, Informed consent, misconduct, data fabrication and/or falsification, double publication and/or submission, redundancy, etc) have been completely observed by the authors.

References

1. Khaniabadi YO, Polosa R, Chuturkova RZ, Daryanoosh M, Goudarzi G, Borgini A, et al. Human health risk assessment due to ambient PM_{10} and SO_2 by an air quality modeling technique. Process Safety and Environmental Protection. 2017;111:346–354. Available from: https://doi.org/10.1016/j.psep.2017.07.018

2. Liu Q, Weng J, Li C, Feng Y, Xie M, Wang X, et al. Attenuation of $PM_{2.5}$-induced alveolar epithelial cells and lung injury through regulation of mitochondrial fission and fusion. Particle and Fibre Toxicology. 2023;20(1):28.

3. Hayakawa K, Tang N, Nagato EG, Toriba A, Sakai S, Kano F, et al. Long term trends in atmospheric concentrations of polycyclic aromatic hydrocarbons and nitropolycyclic aromatic hydrocarbons: A study of Japanese cities from 1997 to 2014. Environmental Pollution. 2018;233:474–482. Available from: https://doi.org/10.1016/j.envpol.2017.10.038

4. Nowakowski M, Rykowska I, Wolski R, Andrzejewski P. Polycyclic Aromatic Hydrocarbons (PAHs) and their Derivatives (O-PAHs, N-PAHs, OH-PAHs): Determination in Suspended Particulate Matter (SPM) – a Review. Environmental Processes [Internet]. 2022;9(1):2. Available from: https://doi.org/10.1007/s40710-021-00555-7

5. Tuerxunbieke A, Xu X, Pei W, Qi L, Qin N, Duan X. Development of Phase and Seasonally Dependent Land-Use Regression Models to Predict Atmospheric PAH Levels. Toxics. 2023;11(316):1–15. Available from: https://doi.org/10.3390/toxics11040316

6. Azhari A. Polycyclic aromatic hydrocarbons (pahs) in air and vegetation: Case study at three selected toll stations along north south expressway in Johor, Malaysia (Doctoral dissertation, Universiti Tun Hussein Onn Malaysia). 2012.

7. Jang E, Alam MS, Harrison RM. Source apportionment of polycyclic aromatic hydrocarbons in urban air using positive matrix factorization and spatial distribution analysis. Atospheric Environment. 2013;79:271–285. Available from: http://dx.doi.org/10.1016/j.atmosenv.2013.06.056

8. Kamal A, Cincinelli A, Martellini T, Malik RN. Linking mobile source-PAHs and biological effects in traffic police officers and drivers in Rawalpindi (Pakistan). Ecotoxicology and Environmental Safety. 2016;127:135–143. Available from: http://dx.doi.org/10.1016/j.ecoenv.2016.01.006

9. Gupta S, Kumar K, Srivastava A, Srivastava A, Jain VK. Size distribution and source apportionment of polycyclic aromatic hydrocarbons (PAHs) in aerosol particle samples from the atmospheric environment of Delhi, India. Science of the Total Environment. 2011;409(22):4674–4680. Available from: http://dx.doi.org/10.1016/j.scitotenv.2011.08.008

10. Wnorowski A, Harnish D, Jiang Y, Celo V, Dabek-Zlotorzynska E, Charland JP. Assessment and Characterization of Alkylated PAHs in Selected Sites across Canada. Atmosphere. 2022;13(1320):1–16. Available from: https://doi.org/10.3390/atmos13081320

11. McGrath JA, Joshua N, Bess AS, Parkerton TF. Review of Polycyclic Aromatic Hydrocarbons (PAHs) Sediment Quality Guidelines for the Protection of Benthic Life. Integrated Environmental Assessment and Management. 2019;15(4):505–518. Available from: https://doi.org/10.1002/ieam.4142

12. Borrás E, Tortajada-Genaro LA, Vázquez M, Zielinska B. Polycyclic aromatic hydrocarbon exhaust emissions from different reformulated diesel fuels and engine operating conditions. Atmospheric Environment. 2009;43(37):5944–5952.

13. Pedersen PS, Ingwersen J, Nielsen T, Larsen E. Effects of Fuel, Lubricant, and Engine Operating Parameters on the Emission of Polycyclic Aromatic Hydrocarbons.

Environmental Science and Technology. 1980;14(1):71–9. Available from: https://doi.org/10.1021/es60161a011

14. Bari CS, Navandar Y V., Dhamaniya A. Vehicular Emission Modeling at Toll Plaza Using Performance Box Data [Internet]. Vol. 24, Journal of Hazardous, Toxic, and Radioactive Waste. 2020 Oct 1;24(4):05020003. Available from: https://doi.org/10.1061/(ASCE)HZ.2153-5515.0000550

15. Nazneen, Patra AK, Kolluru SSR, Dubey R, Kumar S. Occupational exposure to respirable and diesel particulate matter at a highway toll station in India. International Journal of Environmental Science and Technology. 2023;21(1):341–358. Available from: https://doi.org/10.1007/s13762-023-04853-5

16. Karjalainen P, Pirjola L, Heikkilä J, Lähde T, Tzamkiozis T, Ntziachristos L, et al. Exhaust particles of modern gasoline vehicles: A laboratory and an on-road study. Atmospheric Environment. 2014;97:262–270. Available from: https://doi.org/10.1016/j.atmosenv.2014.08.025

17. Coelho MC, Farias TL, Rouphail NM. Measuring and Modeling Emission Effects for Toll Facilities. Transportation Research Record 1941. 2005;136–44.

18. Millo F, Vlachos T, Piano A. Physicochemical and mutagenic analysis of particulate matter emissions from an automotive diesel engine fuelled with fossil and biofuel blends. Fuel. 2021;285:1–10. Available from: https://doi.org/10.1016/j.fuel.2020.119092

19. Matti Maricq M. Chemical characterization of particulate emissions from diesel engines: A review. Journal of Aerosol Science. 2007;38(11):1079–1118. Available from: https://doi.org/10.1016/j.jaerosci.2007.08.001

20. Karavalakis G, Short D, Vu D, Villela M, Asa-awuku A, Durbin TD. Evaluating the regulated emissions , air toxics , ultrafine particles , and black carbon from SI-PFI and SI-DI vehicles operating on different ethanol and iso-butanol blends. FUEL. 2014;128:410–421. Available from: http://dx.doi.org/10.1016/j.fuel.2014.03.016

21. Blanquart G, Pitsch H. Thermochemical properties of polycyclic aromatic hydrocarbons (PAH) from G3MP2B3 calculations. 5th US Combustion Meeting 2007. 2007;6:3764–3783.

22. Zhang Q, Gao M, Sun X, Wang Y, Yuan C, Sun H. Nationwide distribution of polycyclic aromatic hydrocarbons in soil of China and the association with bacterial community. Journal of Environmental Sciences. 2023;128:1–11. Available from: https://doi.org/10.1016/j.jes.2022.07.026

23. Wang W, Massey Simonich SL, Xue M, Zhao J, Zhang N, Wang R, et al. Concentrations, sources and spatial distribution of polycyclic aromatic hydrocarbons in soils from Beijing, Tianjin and surrounding areas, North China. Environmental Pollution. 2010;158(5):1245–1251. Available from: https://doi.org/10.1016/j.envpol.2010.01.021

24. Cheruyiot NK, Lee WJ, Mwangi JK, Wang LC, Lin NH, Lin YC, et al. An overview: Polycyclic aromatic hydrocarbon emissions from the stationary and mobile sources and in the ambient air. Aerosol and Air Quality Research. 2015;15(7):2730–2762. Available from: https://doi.org/10.4209/aaqr.2015.11.0627

25. Phan Thi LA, Ngoc NT, Quynh NT, Thanh N Van, Kim TT, Anh DH, et al. Polycyclic aromatic hydrocarbons (PAHs) in dry tea leaves and tea infusions in Vietnam: contamination levels and dietary risk assessment. Environmental Geochemistry and Health. 2020;42(9):2853–2863. Available from: https://doi.org/10.1007/s10653-020-00524-3

26. Agudelo-Castañeda D, Teixeira E, Schneider I, Lara SR, Silva LFO. Exposure to polycyclic aromatic hydrocarbons in atmospheric $PM_{1.0}$ of urban environments: Carcinogenic and mutagenic respiratory health risk by age groups. Environmental Pollution. 2017;224:158–170. Available from: https://doi.org/10.1016/j.

envpol.2017.01.075

27.   Dzier K, Popek R, Gawro H. Deposition of Particulate Matter of Different Size Fractions on Leaf Surfaces and in Waxes of Urban Forest Species. International Journal of Phytoremediation. 2011;13:1037–1046.

28.   Peng C, Ouyang Z, Wang M, Chen W, Jiao W. Vegetative cover and PAHs accumulation in soils of urban green space. Environmental Pollution. 2012;161:36–42. Available from: http://dx.doi.org/10.1016/j.envpol.2011.09.027

29.   CPCB. Indian Standard Methods for measurment air pollution part 4 suspended-particulate matter. 1999. Available from: https://law.resource.org/pub/in/bis/S02/is.5182.04.1999.pdf

30.   USEPA. Compendium of Methods for the Determination of Toxic Organic Compounds in Ambient Air. In: Determination of Polycyclic Aromatic Hydrocarbons (PAHs) in Ambient Air Using Gas Chromatography/Mass Spectrometry (GC/MS). 1999. Available from: https://www.epa.gov/amtic/compendium-methods-determination-toxic-organic-compounds-ambient-air

31.   U.S. EPA. Compendium Method IO-3.1: Selection, preparation and extraction of filter material [Internet]. Compendium of Methods for the Determination of Inorganic Compounds in Ambient Air EPA/625/R-96/010a Compendium Method IO-3.1 SELECTION,. 1999. Available from: https://www.epa.gov/sites/default/files/2015-07/documents/epa-io-3.1.pdf

32.   U.S. EPA. Compendium of Methods for the Determination of Inorganic Compounds in Ambient Air. Determination of metals in ambient particulate matter using X-Ray Fluorescence (XRF) Spectroscopy. 1999. Available from: http://www3.epa.gov/ttnamti1/files/ambient/inorganic/mthd-3-3.pdf

33.   CPCB. Indian Standard method for measurment of air pollution part 12 polynuclear aromatic hydrocarbons (PAHs) in air p-articulate matter. 2004. Available from: https://law.resource.org/pub/in/bis/S02/is.5182.12.2004.pdf

34.   Khan ZA, Hellier P, Ladommatos N. Measurement of soot mass and PAHs during the pyrolysis of C2–C4 alcohols at high temperatures. Combustion and Flame. 2022;236:1–15. Available from: https://doi.org/10.1016/j.combustflame.2021.111803

35.   U.S. Environmental Protection Agency. Quality Assurance Systems Pollution Measurement Handbook for Air Volume. Vol. II. 2017. Available from: https://www.epa.gov/sites/default/files/2020-10/documents/final_handbook_document_1_17.pdf

36.   Fasani D, Fermo P, Barroso PJ, Martín J, Santos JL, Aparicio I, et al. Analytical Method for Biomonitoring of PAH Using Leaves of Bitter Orange Trees (Citrus aurantium): a Case Study in South Spain. Water, Air, & Soil Pollution [Internet]. 2016;360:1–11. Available from: http://dx.doi.org/10.1007/s11270-016-3056-z

37.   Ravindra K, Sokhi R, Van Grieken R. Atmospheric polycyclic aromatic hydrocarbons: Source attribution, emission factors and regulation. Atmospheric Environment. 2008;42(13):2895–921. Available from: https://doi.org/10.1016/j.atmosenv.2007.12.010

38.   WHO. Air quality guidelines for Europe ; second edition. 2019. Available from: https://www.who.int/publications/i/item/9789289013581

39.   Yin H, Xu L. Comparative study of $PM_{10}/PM_{2.5}$-bound PAHs in downtown Beijing, China: Concentrations, sources, and health risks. Journal of Cleaner Production. 2018;177:674–83. Available from: https://doi.org/10.1016/j.jclepro.2017.12.263

40.   Yang L, Zhang X, Xing W, Zhou Q, Zhang L, Wu Q, et al. Yearly variation in characteristics and health risk of polycyclic aromatic hydrocarbons and nitro-PAHs in urban shanghai from 2010–2018. Journal of Environmental Sciences (China). 2021;99:72–79. Available from: https://doi.org/10.1016/j.jes.2020.06.017

41.   Ali M, Athar M. Air pollution due

to traffic, air quality monitoring along three sections of National Highway N-5, Pakistan. Environmental Monitoring and Assessment. 2008;136(1–3):219–26. Available from: https://doi.org/10.1007/s10661-007-9677-3

42.　Pant P, Harrison RM. Estimation of the contribution of road traffic emissions to particulate matter concentrations from field measurements: A review. Atmospheric Environment. 2013;77:78–97. Available from: http://dx.doi.org/10.1016/j.atmosenv.2013.04.028

43.　Ceratti AM, Marques G, Alves DD, Cansi M, Hansen J, Brochier F, et al. Polycyclic Aromatic Hydrocarbons (PAH) in Atmospheric of the Environmental Scenario in Urban Areas. Water, Air, & Soil Pollution. 2021;232(30):1–17. Available from: https://doi.org/10.1007/s11270-020-04967-3

44.　Teixeira EC, Mattiuzi CDP, Agudelo-Castañeda DM, De Oliveira Garcia K, Wiegand F. Polycyclic aromatic hydrocarbons study in atmospheric fine and coarse particles using diagnostic ratios and receptor model in urban/industrial region. Environmental Monitoring and Assessment. 2013;185(11):9587–9602. Available from: https://doi.org/10.1007/s10661-013-3276-2

45.　Gunawardena J, Egodawatta P, Ayoko GA, Goonetilleke A. Role of traffic in atmospheric accumulation of heavy metals and polycyclic aromatic hydrocarbons. Atmospheric Environment. 2012;54:502–510. Available from: http://dx.doi.org/10.1016/j.atmosenv.2012.02.058

46.　Rafaela P, Lucio S, Ferreira F, Perin E, Mirna M, Farias F De, et al. Traffic-related polycyclic aromatic hydrocarbons (PAHs) occurrence in a tropical environment. Environmental Geochemistry and Health. 2021;43(11):4577–4587. Available from: https://doi.org/10.1007/s10653-021-00947-6

47.　Barreca S, Bastone S, Caponetti E, Martino DFC, Orecchio S. Determination of selected polyaromatic hydrocarbons by gas chromatography-mass spectrometry for the analysis of wood to establish the cause of sinking of an old vessel (Scauri wreck) by fire. Microchemical Journal. 2014;117:116–121. Available from: http://dx.doi.org/10.1016/j.microc.2014.06.020